Al Najm *Iraqi Journal of Science, 2020, Vol. 61, No. 5, pp: 1233-1243*
DOI: 10.24996/ijs.2020.61.5.30

ISSN: 0067-2904

Studying the Atomic and Molecular Hydrogen Mass (MHI, MH_2) Properties of the Extragalactic Spectra

M. N. Al Najm
Department of Astronomy and Space, College of Science, University of Baghdad, Baghdad, Iraq

Received: 5/8/ 2019 Accepted: 30/9/2020

Abstract

The purpose of this study is to deal with dust and interstellar molecular and atomic gas owing to obtaining a proportion of cold gas to dust and to understand the characteristics of the molecular gas in extragalactic data selected from the Herschel SPIRE/ FTS archive. The physical properties of a sample of 65 extragalactic spectra characterized by the activity of star formation were discussed in this work. Statistical analyses, using STATISTICA program, were made for the content of cold gas (MHI, MH_2), dust mass (M_{dust}), cold temperature of dust (T_d) and luminosities in Far-infrared to CO line radiations, while coefficients of partial correlation within those characteristics were established. The results showed that the molecular hydrogen mass (MH_2) is strongly correlated with the HI or the total gas mass corresponding to the Far-infrared emission (L_{FIR}) resulting from dust in the galaxies molecular clouds. The results also indicated that these kinds of galaxies have large molecular mass as well as high star formation efficiency per unit mass.

Keywords: Galaxies; Interstellar gas; Molecular clouds; Far-Infrared and CO line radiations.

دراسة خصائص كتلة الهيدروجين الذري والجزيئي (MH_2،MHI) لأطياف المجرات الخارجية

محمد ناجي ال نجم
قسم الفلك والفضاء، كلية العلوم، جامعة بغداد، بغداد، العراق

الخلاصه

ان الغرض من هذه الدراسة هو التعامل مع الغبار والغازات الجزيئية والذرية ما بين النجوم وذلك للحصول على نسبة الغاز البارد إلى الغبار وفهم خصائص الغاز الجزيئي من بيانات المجرات الخارجية المختارة من أرشيف Herschel SPIRE / FTS. في هذا العمل تمت مناقشة الخواص الفيزيائية لعينة 65 من أطياف المجرات الخارجية والتي تتميز بفعالية النشوء النجمي. تم إجراء التحليلات الإحصائية لمحتوى الغاز البارد (MHI,MH_2)، وكتلة الغبار (M_{dust}) ودرجة الحرارة الباردة للغبار (T_d) وضيائيات الأشعة تحت الحمراء البعيدة إلى إشعاعات خط اول اوكسيد الكاربون CO، وتم تحديد معاملات الارتباط الجزئي ضمن تلك الخصائص. التحليلات الإحصائية حصلت عليها باستخدام برنامج STATISTICA. اظهرت النتائج أن كتلة الهيدروجين الجزيئي (MH_2) ترتبط ارتباطًا قوياً مع كتلة الهدروجين الذري HI أو كتلة الغاز الكلية المقابلة لانبعاث الأشعة تحت الحمراء البعيدة (L_{FIR}) الناتج من الغبار الموجود في السحب الجزيئية للمجرات. اشارت النتائج أيضًا إلى أن هذه الأنواع من المجرات تمتلك كتلة جزيئية كبيرة اضافة الى كفاءة نشوء نجمي عالية لكل وحدة كتلة.

*Email: mohalnajm72@yahoo.com

Introduction

Galaxies throughout all environments can possess a cold gas component suitable for powering star formation or an active galactic nucleus (AGNs). Studies of local universe galaxies demonstrated that many of them contain important nuclear and molecular cold gas reservoirs [1]. The molecular gas within the multi-phase interstellar medium (ISM) was the most closely tied to star formation rate (SFR), and thus dramatic effects on galaxies evolution are associated with the stellar lifecycle. Even if the dominant component of such gas is molecular hydrogen (H2), it is difficult to detect pure H2 rotational lines without being especially sensitive to the cold temperatures of most molecular clouds [2]. The star formation efficiency (SFE) is a crucial component in understanding the history of star formation of galaxies at all redshifts as well as the universe's global evolution [3].

The poor understanding of the physical principles behind the star formation process still restricts our knowledge of galaxies evolution, in other words, the condensation of the primitive gaseous material of HI into H_2 and thus its collapse into stars. The feedback mechanisms caused by the recently born stars on the ISM are also poorly known. The ultraviolet emission field (UVWF) linked with massive star formation causes the nearby gas to be ionized and leads the hydrogen molecules to be photo-dissociated. Supernova winds, furthermore, inject kinetic energy (and metals) into the ISM, causing unique star formation on the shock wave fronts [4]. Far-infrared radiations in these sources are primarily caused by ultraviolet (UV) emission-warmed dust from young and gigantic stars in the neighbor galaxies [5]. A previous study [6] illustrated that massive envelopes of extragalactic emission's ionized hydrogen (HII) with masses that are significantly surpassing the masses of intergalactic HI disks could exist across galaxies in which the dimensions of HI disks exceed those of stellar disks considerably. These enlarged disks could in considerable time scales "feed" the formation rate of stars in their host galaxies. According to a published article [7], the nuclei of active galaxies that are contiguous to molecular gas tend to have considerably redder infrared colors and they cause a lack in molecules of carbon monoxide (CO) detections, revealing duster environments in the CO luminous nuclei.

Evolution observations in the dust-to-metal ratio enable us to restrict the processes of the prevailing dust processing [8]. The forms of HI H_2 are well linked with previous and present indices of star formation rate, such as the brightness of the surface of the blue F_B, Far-infrared F_{FIR} and radio continuum F_R, but the correlation is stronger for the molecular clouds content of MH_2 [9], indicating increased molecular hydrogen gas excitation. Findings related to the dust and the atomic and molecular gas mass of these galaxies enable us to investigate their star formation activity and obtain their interstellar gas properties.

This paper is structured according to the following: We describe the characteristics of our observational data details of the 65 extragalactic samples and procedures to evaluate all parameters in Section 2. The results and discussion of our statistical analysis are presented in Section 3. The conclusions drawn from this study are given in Section 4.

Observations Sample and Description Parameters

Sample Selection

The cold gas (atomic + molecular) kinematics for 65 extragalactic spectra samples from an archive of the Herschel SPIRE Fourier Transform Spectrometer (FTS) were studied by means of the statistical analysis of the MH_2+HI masses properties. In particular, cold gas masses-to-luminosities relations of SPIRE observations of the galaxies were studied extensively. The limited parameters (for example; galaxy name, Far-infrared luminosity L_{FIR} and distance luminosity D_l) were extracted from new observations of a recent paper [2], while the redshifts of galaxies measured by Doppler-shifted (z), Far-infrared fluxes at 60 μm and 100 μm (F_{60} and F_{100} μm) were taken from NASA/IPAC Extragalactic Database (NED) [10]. The calculated parameters (name galaxy, Log L_{FIR}, D_l, z, F_{60}, and F_{100}) of each selected galaxy are listed in Table-1.

Table 1- Data obtained from [2] and NASA/IPAC Extragalactic (NED) of the parameters used in our analysis.

No.	*Name Galaxy*	$LogL_{FIR}$ (L_{Θ})	D_l (Mpc)	*z*	*F60* (Jy)	*F100* (Jy)	*Morphological Type*
1	NGC 0023	10.9	68	0.01524	9.03	15.66	Sa
2	NGC 34	11.2	85	0.02000	17.05	16.86	S0-a
3	IRAS 00188-0856	12.2	591	0.12800	2.592	3.403	Galaxy or QSO*
4	ESO 350-IG038	10.8	87	0.02100	6.88	5.04	Irr**
5	IRAS 00397-1312	12.6	1285	0.26100	1.832	1.904	Galaxy or QSO
6	NGC 0232	11.2	95	0.02300	10.05	15.75	SBa
7	NGC 253	10.3	3	0.00100	967.81	1288.15	SABc
8	I Zw 1	11.4	272	0.06000	2.161	1.749	Sc
9	NGC 0317B	11	80	0.01771	9.34	13.95	SBbc
10	IRAS 01003-2238	11.9	539	0.11800	2.287	1.79	Galaxy or QSO
11	IC 1623	11.4	86	0.01900	23.85	31.53	S?
12	ESO 244-G012	11.1	95	0.022903	9.27	11.76	Sc
13	CGCG 436-030	11.5	138	0.03100	10.71	9.67	Sbc
14	Mrk 1014	12.3	763	0.16300	2.348	1.915	Galaxy or QSO
15	NGC 0828	11.1	80	0.017926	11.46	25.33	Sa
16	NGC 0891	10.2	10	0.00176	66.46	172.23	Sb
17	UGC 01845	10.9	70	0.01514	10.31	15.51	Sab
18	NGC 0958	10.9	82	0.01915	5.85	15.08	SBc
19	NGC 1056	9.7	24	0.005154	5.33	10.2	Sa
20	NGC 1097	10.4	16	0.00424	58.29	116	SBb
21	IRAS 03158+4227	12.4	623	0.13400	4.256	4.276	Galaxy or QSO
22	3C 84	10.8	78	0.01756	7.09	7.6	S0
23	NGC 1482	10.5	25	0.006206	33.36	46.73	S0-a
24	IRAS 03521+0028	12.3	709	0.15191	2.638	3.833	Galaxy or QSO
25	UGC 02982	10.9	77	0.01771	8.38	16.82	SABa
26	ESO 420-G013	10.7	49	0.01191	13.66	20.88	S0-a
27	NGC 1572	11	86	0.020394	8.03	16.81	SBa
28	NGC 1614	11.3	68	0.01600	32.12	34.32	SBc
29	UGC 03094	11.1	108	0.02470	6.35	12.85	Sab
30	MCG-05-12-006	10.9	78	0.01875	8.15	9.404	SBb
31	IRAS F05189-2524	11.8	185	0.04256	13.25	11.84	E**
32	IRAS09022-3615	12	411	0.05960	11.64	11.08	Galaxy or QSO
33	NGC 2764	10	40	0.00907	3.67	7.224	S0

34	M81	9.2	4	0.00090	6.806	32.03	Sab
35	NGC 3077	7.7	1	0.00005	15.9	26.53	S?
36	NGC 3221	10.7	61	0.01370	7.72	18.76	Sc
37	IRAS F10565+2448	11.8	192	0.04300	12.1	15.01	Irr
38	NGC 3627	10.2	12	0.00243	66.31	136.56	Sb
39	ESO 320-G030	11	45	0.01084	34.38	46.28	SABa
40	NGC 4051	9.5	14	0.00234	10.53	24.93	SABb
41	NGC 4459	9.1	19	0.00396	1.87	4.82	S0
42	NGC 4569	7.5	1	0.00510	9.8	26.56	Sab
43	NGC 4710	9.6	18	0.00375	5.89	13.21	S0-a
44	NGC 4736	9.9	8	0.00105	71.54	120.69	SABa
45	NGC 5010	10.6	43	0.02100	10.29	21.69	S0-a
46	NGC 5104	10.9	82	0.01855	6.78	13.37	Sa
47	IRAS 14378-3651	11.9	303	0.06760	6.72	8.08	Galaxy or QSO
48	NGC 5866	9.4	14	0.00225	5.26	16.98	S0-a
49	IRAS 16090-0139	12.3	618	0.13400	3.609	4.874	Galaxy or QSO
50	PG 1613+658	11.5	600	0.12900	0.635	1.002	E
51	IRAS F16399-0937	11.3	118	0.027012	8.42	14.72	Galaxy or QSO
52	NGC 6240	11.6	108	0.02450	22.94	26.49	S0-a
53	NGC 6701	10.9	62	0.01320	10.05	20.05	Sa
54	IRAS 19254-7245	11.8	270	0.061709	5.16	5.789	Galaxy or QSO
55	IRAS 20100-4156	12.4	595	0.13000	5.19	5.165	Galaxy or QSO
56	MCG+04-48-002	10.9	65	0.01400	8.15	12.5	Sd
57	NGC 6946	9.8	5	0.00015	129.78	290.69	SABc
58	IRAS 20414-1651	12	392	0.08600	4.364	5.247	Galaxy or QSO
59	IC 5063	10.2	46	0.01130	5.87	4.25	S0-a
60	CGCG 448-020	11.7	161	0.03610	12.65	11.76	S0-a
61	NGC 7582	10.5	21	0.00500	52.25	82.86	SBab
62	IRAS 23230-6926	12.1	482	0.10700	3.744	3.42	Galaxy or QSO
63	IRAS 23365+3604	12	290	0.06450	7.44	9.01	Galaxy or QSO
64	NGC 7771	11.1	63	0.01400	20.93	44.85	Sa
65	Mrk331	11.2	81	0.01848	18.43	22.56	Sa

Note: * *QSO=Quasar and* ** *Irr=Irregular galaxy; E= Ellipticals.*

Statistical procedures

The statistical software ,statistic-win-program, was utilized to process and analyze various relationships between variables and calculate whether toughness of regression exists between the behaviors of the two variables. This association is also represented in the form of scattering graphs. The linear partial correlation (R) coefficient values range from + 1 to -1 [11, 12]. A regression value of ±1 refers that the two functions are perfectly correlated. Indeed, when the value of the measurement of R is or close to zero, there is a weak regression correlation between the two components.

Description Parameters

In general, the term luminosity of the CO line was calculated from the integrated intensity S_{co} in Jy Km s^{-1}, and beam solid angle $\Omega_b = \pi\theta_B^2/4ln2$ $(\theta_B\ in\ radians)$. The CO line luminosity can be found by [13, 14]:

$$L_{co} = \frac{\Omega_b S_{co} D_l^{\,2}}{(1+z)^3} \quad (in\ K\ km\, s^{-1} pc^2) \ldots\ldots\ldots\ldots\ldots\ldots (1)$$

where D_l is the distance of cosmological luminosity in megaparsec (Mpc) described by standard cosmological parameters including Hubble constant H_0, matter density parameter Ω_M, and a parameter of cosmological constant density Ω_Λ, and can be determined by [13]:

$$D_l = (1+z)\frac{c}{H_0}\int_0^z \frac{dz}{[\Omega_M(1+z)^3 + \Omega_\Lambda]^{1/2}} \ldots\ldots\ldots\ldots\ldots (2)$$

By substituting equation (2) in equation (1), the CO line luminosity (L_{co}) takes the form:

$$L_{co} = (\frac{c}{H_0})^2 \frac{\Omega_b S_{co}}{(1+z)} \cdot \frac{z}{[\Omega_M(1+z)^3 + \Omega_\Lambda]^{1/2}} \ldots\ldots\ldots\ldots\ldots (3)$$

where c is the speed of light.

For galaxies without strong interactions, the following relationship between L_{FIR} and L_{CO} is constructed by [15, 16]:

$$\frac{L_{FIR}}{10^9} L_{\Theta} = 31[\frac{L_{co}}{10^9} L_{\Theta}]^{0.74} \ldots\ldots\ldots\ldots\ldots\ldots\ldots (4)$$

and could be written in the form:

$$[\frac{(L_{FIR}\ /10^9)L_{\Theta}}{31}]^{1.35} = \frac{L_{co}}{10^9} L_{\Theta} \ldots\ldots\ldots\ldots\ldots\ldots\ldots (5)$$

The logarithmic scale of equation (5) is written as:

$$LogL_{co} = 1.35LogL_{FIR} - 5.2 \ldots\ldots\ldots\ldots\ldots\ldots\ldots (6)$$

Here Lco and L_{FIR} are given in the solar luminosity unit (L_{Θ}).

The molecular hydrogen gas mass MH_2 in solar mass (M_{Θ}) is derived with the use of the formula [14-17]:

$$MH_2(M_\odot) = \alpha_{CO} L_{co}(L_\odot) \ldots\ldots\ldots\ldots\ldots\ldots\ldots (7)$$

where α_{CO} is the CO line luminosity-to- molecular gas mass conversion factor. The conversion factor α_{CO} is almost constant and equal to $\alpha_{CO} \approx 0.6 - 5$ in unit M_{Θ} (K km s^{-1} pc^2)$^{-1}$ [14-19]. The value of α_{CO} that is used in this study is ~ 4.8 M_{Θ} (K km s^{-1} pc^2)$^{-1}$ [15-17].

From equations 6 and 7, we have:

$$Log\ MH_2(in\ unit\ M_\odot) = 1.35 \log L_{FIR}(L_{\Theta}) - 4.5 \ldots\ldots\ldots\ldots (8)$$

4- The logarithmic scale of MHI in M_{Θ} can be calculated as follows [15]:

$$Log\ MHI(in\ unit\ M_\odot) = 0.61 \log L_{FIR}(L_{\Theta}) + 3.08 \ldots\ldots\ldots\ldots (9)$$

The dust temperature T_d in (K^0) is given roughly by [20, 21]:

$$T_d \approx 49(\frac{F_{60\mu m}}{F_{100}\mu m})^{0.4} \ldots\ldots\ldots\ldots\ldots\ldots\ldots (10)$$

where F_{60} μm and F_{100} μm are IRAS Far- infrared band fluxes at 60 μm and 100 μm in unit Jansky (Jy), where 1 Jy= 10^{-26} $W.m^{-2}.Hz^{-1}$ (in units SI).

The dust mass of galaxies M_{dust} in the solar mass unit can be estimated by integrating the temperature database with the Far-infrared flux rates of F60 μm and F100 μm [20, 22]:

$$M_{dust}\ (M_{\Theta}) = 0.00478. F_{100}(mJy). D_l^{\,2}. \left\{ e^{\left[2.94\left(\frac{F_{100\mu m}}{F_{60\mu m}}\right)^{0.4}\right]} - 1 \right\} \ldots\ldots\ldots (11)$$

We can re-write equation (10) as:

$$(\frac{F_{100\mu m}}{F_{60\mu m}})^{0.4} = \frac{49}{T_d}$$

The substitution of the term $\frac{49}{T_d}$ instead of $(\frac{F_{100\mu m}}{F_{60\mu m}})^{0.4}$ in equation (11) yields:

$$M_{dust}\ (M_{\Theta}) = 4.78F_{100}(Jy)\ D_l^{\,2}\{e^{144/T_d} - 1\} \ldots\ldots\ldots\ldots\ldots\ldots\ldots. (12)$$

7- The star formation rate (SFR) is calculated in Far-infrared bands (60-100 μm) from the relation [23]:

$$SFR_{FIR} = \left(\frac{L_{FIR}}{5.7 * 10^9\ \ L_{\Theta}}\right) \quad (in\ M_{\Theta}\ yr^{-1}) \ldots\ldots\ldots\ldots\ldots\ldots\ldots\ldots\ldots\ldots\ldots. (13)$$

8- Lifetime gas depletion (t_{gas}) which is usually measured in years and caused by high mass star formation (without mass recycling by supernovae or other mass losses) is calculated as follows [16]:

$$t_{gas} = 5 * 10^{10}\left(\frac{L_{co}}{L_{FIR}}\right) \quad (in\ unit\ yr) \ldots\ldots\ldots\ldots\ldots\ldots\ldots\ldots\ldots\ldots\ldots\ldots. (14)$$

Results and Discussion

This work studied the relationships between Far-infrared, CO emission line luminosities, star formation rates in the Far-infrared band and masses of atomic hydrogen (MHI)+molecular hydrogen (MH_2) of a *Herschel SPIRE FTS* galaxies sample. The results of the comparison between the cold gas content and luminosities revealed different effects.

The results of statistical analysis showed that the mean value ± standard error of LogL_{FIR} is equal to 10.93 ± 0.12 (L_{FIR}=8.5x10^{10} L_{Θ}) for our sample galaxies. These galaxies have a higher Far-infrared luminosity with a lower limit of about ≈ 3.2x$10^{10}L_{\Theta}$ and an upper quartile which is equal to 5x$10^{11}L_{\Theta}$. The calculations showed a very strong relationship $L_{FIR}\ \alpha\ (MHI+MH_2)^{1.11\pm0.024}$ with a very strong positive partial correlation coefficient (R=0.98) and a very high probability level ($p \leq 10^{-7}$), where p is the probability of chance correlation. Figure-1a shows that the slope is linear and steeper than unity. This study also revealed that the total mass of cold gas (MHI+MH_2) and CO/ FIR luminosities, along with their relative H_2 and HI content alone, are the factors that indicate the actual meaning of the gas.

The relationships among the logarithm dust mass, L_{co}/L_{FIR} ratio, and MHI+MH_2 of theses galaxies were studied. The statistical analysis results showed significant relationships between (Log L_{co}/L_{FIR} , Log M_{dust}) and Log (MHI+MH_2) with a very strong partial correlation coefficient (R≈1) and a very high probability ($p \leq 10^{-7}$), where Figure-1b reveals that the slope is almost linear (Slope > 1). The L_{co} to L_{FIR} ratio provides a qualitative measure of star formation activity in the interaction of galaxies, where the average value < L_{co}/L_{FIR} > =0.05. These galaxies have higher infrared luminous than CO emission. We can conclude that CO emissions will be very essential for studying the central region's gas kinematics and dynamics. Thus, the star formation rate is related to the total gas mass of galaxies.

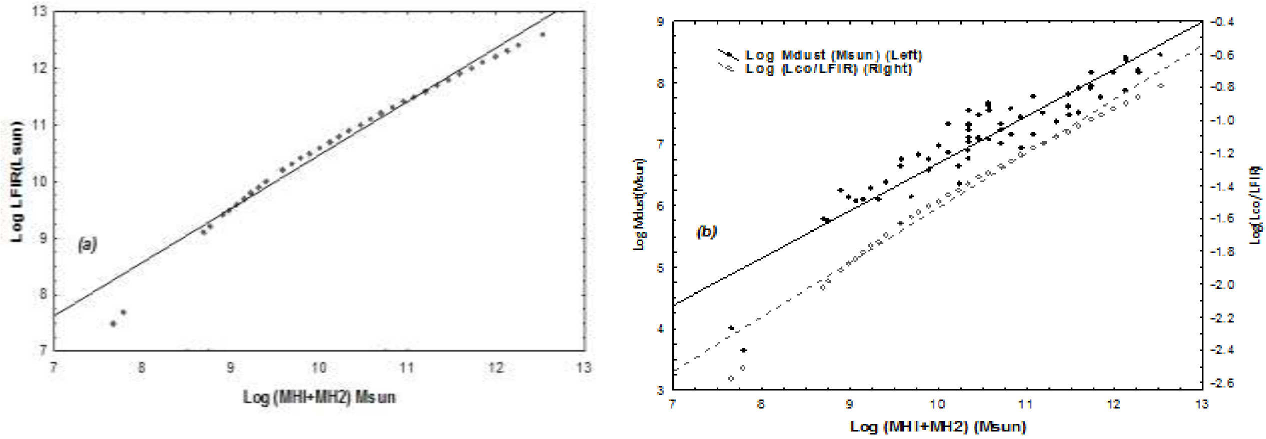

Figure 1- ***(a)*** Far-Infrared luminosity Log L_{FIR} as a function of total cold gas (MHI+MH2), in solar units. The solid line represents the linear correlation regression. ***(b)*** The relationship between dust mass of galaxies M_{dust} (on the left), ratio L_{CO}/L_{FIR} (on the right) and MHI+MH_2. The straight black line represents the fitting to all the data for M_{dust} and the dashed line represents the fitting to the all data for L_{CO}/L_{FIR} versus MHI+MH_2, respectively.

Figure-2a (left panel) demonstrates that the ratio Log (L_{FIR}/MH_2) and dust temperature Figure-2a (left panel) demonstrates that ratio Log (L_{FIR}/MH_2) and dust temperature (T_d) indicate a clear negative relationship with a correlation coefficient of (R≈ -0.46) and a good probability value ($p \approx 10^{-4}$). It should be pointed out here that the slope of the line is ≈ 0.4±0.09. The value of the ratio of Far-infrared emission luminosity to molecular gas implies that the SFR strongly depends on the dust temperature (T_d). The significant relationship between L_{FIR}/MH_2 ratio and T_d supports essentially that the Far-infrared emission comes from the merged dust with the molecular clouds.

The mean values of the logarithmic scale of cold gas masses (MHI, MH_2) of our sample were 9.75±0.08, 10.26±0.17, and 7.06±0.11, whereas those for the M_{dust} were $5.6 \times 10^9\, M_\odot$, $1.8 \times 10^{10}\, M_\odot$, and $1.1 \times 10^9\, M_\odot$, respectively. Figure-2b (right panel) shows a linear relationship, implying that the correlation between molecules gas to dust masses and dust temperature (Log (MH_2/M_{dust}), T_d) is positive and very strong (R≈ 0.87) with a stronger probability ($p \leq 10^{-7}$). The used linear regression equation is given by:

$$\boldsymbol{LogMH_2/M_{dust} = S\, T_d + m},$$

where $\boldsymbol{S}$ is the slope and $\boldsymbol{m}$ is the intercept with the y-axis. It should be noted that the best representation is obtained by a minimum standard error which is clarified in the form of: $LogMH_2/M_{dust} = (0.75 \pm 0.05) T_d + (1.74 \pm 0.27)$. Figure-2b (solid black line), which describes the relationship between (Log MHI/M_{dust}) and (T_d), shows that R≈ 0.45, $p \approx 10^{-4}$, and the slope of the sold line is ≤ 0.5. The comparison between the ratio MHI/M_{dust} and the T_d indicates that the resulted ratio varies from a galaxy to another and that the dust is regarded as an indicator of gas in its atomic and molecular forms.

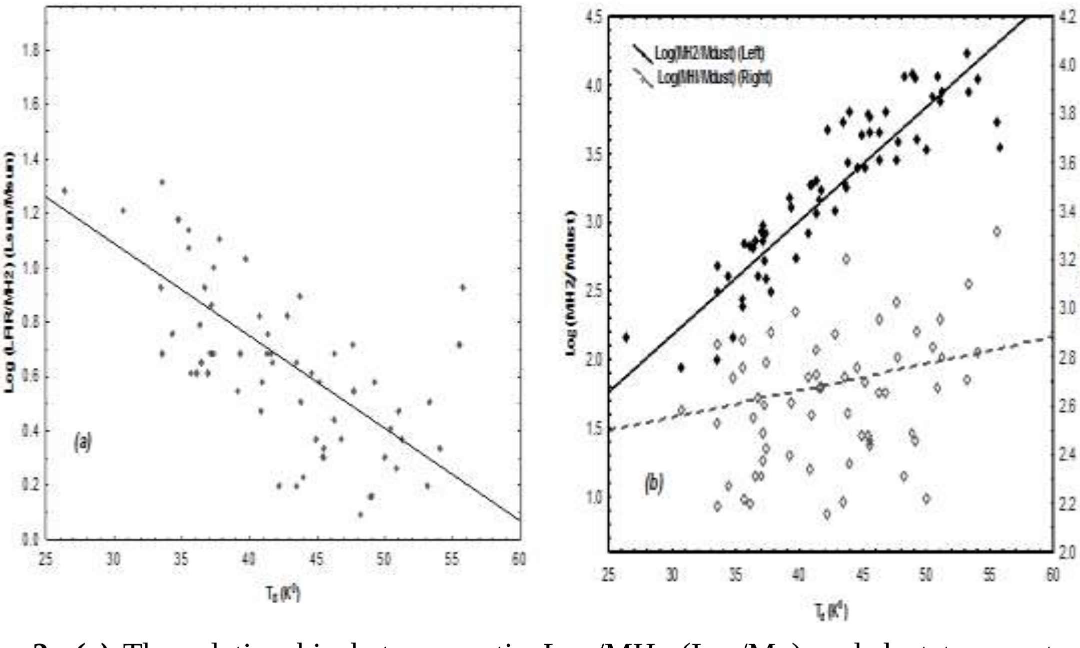

Figure 2- ***(a)*** The relationship between ratio L_{FIR}/MH_2 ($L_\odot / M_\odot$) and dust temperature T_d (K^0). ***(b)*** The relationship between ratios MH_2/M_{dust} (on the left) and MHI/M_{dust} (on the right) as a function of T_d. The straight black line represents the fitting to all the data for MH_2/M_{dust} and the dashed line represents fitting to all the data for MHI/M_{dust} versus T_d.

This work studied the relationship between the ratio masses of molecular hydrogen to dust content (MH_2/M_{dust}) and the Far-infrared luminosity of galaxies. The results of the statistical analysis showed a strong relationship between Log (MH_2/M_{dust}) and Log L_{FIR} with a positive and very strong correlation coefficient (R≈0.84) and a higher probability ($p \leq 10^{-7}$). The ratio MH_2/M_{dust} is used as a function of the Far-infrared luminosity in Figure-3a (left panel), which demonstrates that the relationship is taking the form: ($MH_2/M_{dust}\ \alpha\ L_{FIR}^{0.84 \pm 0.08}$). The ratio MH_2/M_{dust} is also taken as a function of the dust temperature in (Figure-2b left). Both figures showed that the ratio does not depend on the type of morphology of the galaxies, which was also confirmed by previous results [i.e. 7, 15 and 16]. Our results indicate that dust may be associated with the stars emerging in the central bulges of such galaxies, which leads to increasing the dust mass and reducing the cold gas to dust mass ratio.

The relationship between L_{co}/L_{FIR} and T_d, as shown in Figure-3b (right panel), showed a correlation coefficient of R≈ 0.5, probability of $p\approx10^{-4}$, and slope of ~ 0.23 ± 0.06. The results indicate a weak relationship, due to the effect of distance D_l or redshift z based on *Malmquist bias* (the effect of distance dependence selection) between the parameters in this sample (*see equations 1 and 3*).

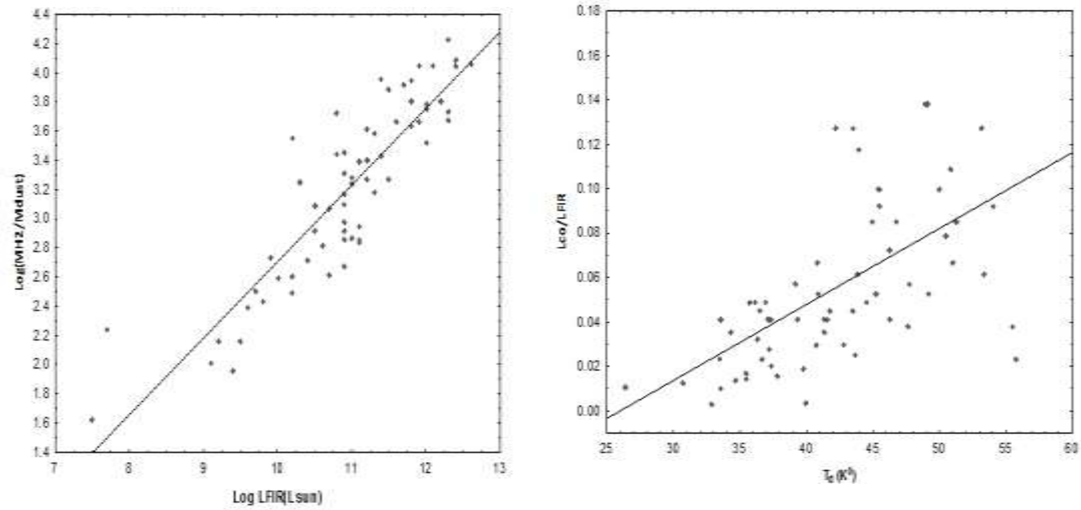

Figure 3-*(a)*The ratio MH_2/M_{dust} as a function of L_{FIR}. ***(b)*** The ratio CO line emission (L_{CO}) to Far-infrared emission (L_{FIR}) luminosities as a function of T_d.

Now we discuss the relationship between the atomic and molecular gas to dust masses and gas depletion lifetime (t_{gas}). It was found that the linear regression of Figure-4a (left panel) is taking the form: *Log* MH_2/M_{dust}= *(1.3±0.15)* t_{gas} *+(2.26±0.09)* while for Figure-4b (right panel) it is: *Log* MH_1/M_{dust}= *(-0.72±0.25)* t_{gas} *+(2.99±0.08)*. There is an interesting relationship between these quantities with a strong positive correlation coefficient (R≈ 0.73) and a very high probability ($p \leq 10^{-7}$) between Log (MH_2/M_{dust}) and t_{gas}. A negative relationship between Log (MHI/M_{dust}) and t_{gas} was also observed, with a partial correlation value of R≈-0.33 and a significance probability ($p=6x10^{-3}$). Based on a sample of extragalactic spectra, we show that the cold gas depletion lifetime is dependent on high star formation efficiency (SFE) with extreme Lco/ L_{FIR} ratio in these galaxies, indicating that the star formation process can only be enhanced by very strong interactions between galaxies.

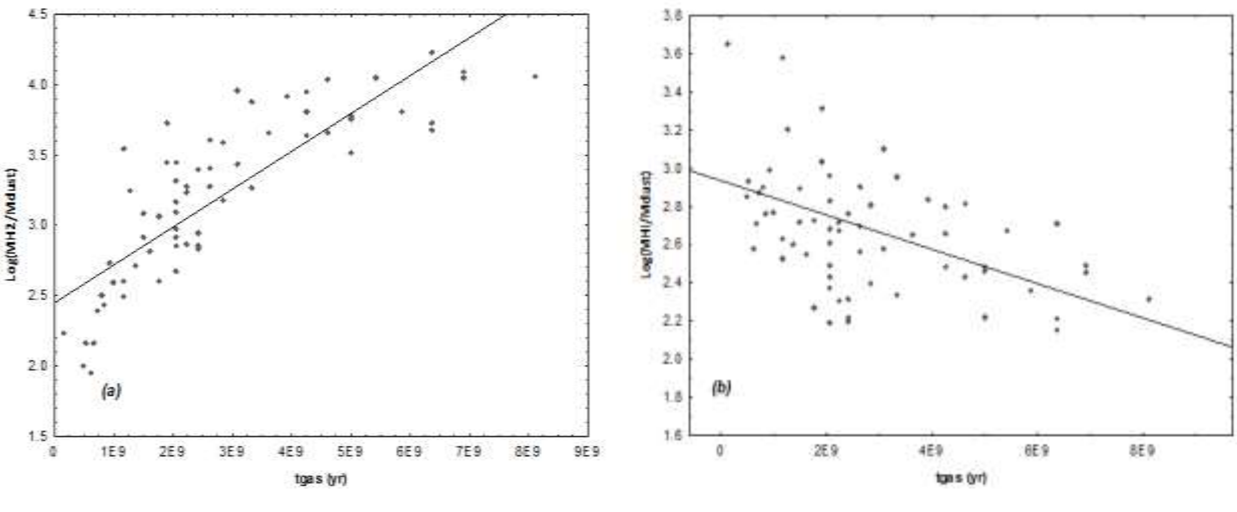

Figure 4- ***(a)*** The ratio MH_2/M_{dust} versus lifetime gas depletion t_{gas} in years unit. ***(b)*** The ratio MHI/M_{dust} versus t_{gas}.

In this work, we also studied the relationships between the mass dust of galaxy (**M_{dust}**) and ratio mass MHI/MH_2, CO-luminosity (**L_{co}**), star formation rate in Far-infrared band (SFR_{FIR}). The results showed mean values of Log MHI/MH_2= -0.51±0.09, LogL_{co}=9.57±0.17 ($L_{co}\approx$ 3.7x10^9 $L_\odot$), and SFR_{FIR}= 44.25 $M_\odot$ yr^{-1} for our sample galaxies. The existence of a negative correlation between MHI/MH_2 ratio and M_{dust} was recorded, with a partial coefficient of R ≈ -0.9. For a slope ≈ -1, we have the LogM_{dust} is inversely proportional to Log (MHI/MH_2). It can also be noticed that if the HI / H_2 ratio mass is less than or equal to 1 (MHI / $MH_2 \leq 1$), there is a systematic variation in the HI content, while the deficiency of MHI as the relative abundance of the molecular component (MH2) increases.

The results also showed a very strong linear correlation between LogL_{co} and LogM_{dust} with a correlation coefficient of R=0.92, a very strong probability ($p \leq 10^{-7}$), and a Slope ~ 0.86±0.04. In terms of statistics, we deduce a tight linear relationship between M_{dust} and SFR_{FIR} (Slope ~ 1). For these galaxies, star formation rate in the Far-infrared radiation band (SFR_{FIR}) is strongly related to their dust content, which is relevant for galaxies involving a wide range of the FIR luminosity. We also found a statistically significant relationship with a clear positive correlation between these parameters (R≈0.5), with a good probability level (p=2x10^{-5}). In Figures-(5a, 5b) and 6, we examine the LogM_{dust} versus Log MHI/MH_2, LogL_{co} versus LogM_{dust}, and M_{dust} versus SFR_{FIR}, respectively. The MH_2 derived from the CO surface brightness is more strongly linked with the M_{dust} than the MHI surface mass, however, the dust mass association of the molecular content is not significant. Therefore, cold dust emission is probably correlated with both of the atomic and molecular forms in these galaxies. In fact, the dust mass is often related to the MHI+MH_2. Our findings from this analysis are consistent with those of previous articles [7, 9, 15, 16].

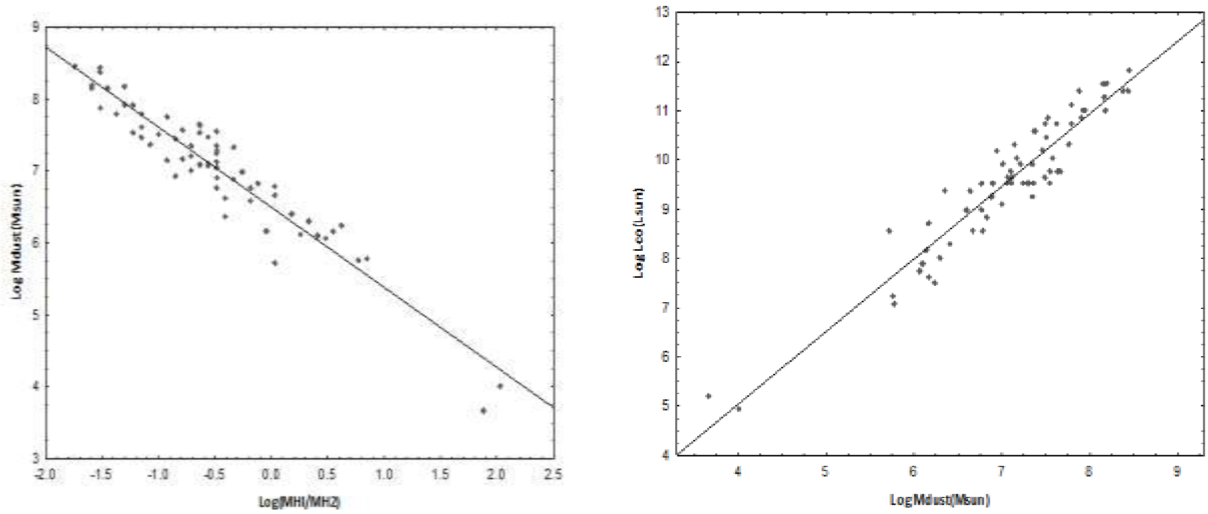

Figure 5- (a) The M_{dust} ($M_\odot$) as a function of the ratio MHI/MH_2. ***(b)*** The CO line luminosity versus M_{dust}, on a scale of logarithms.

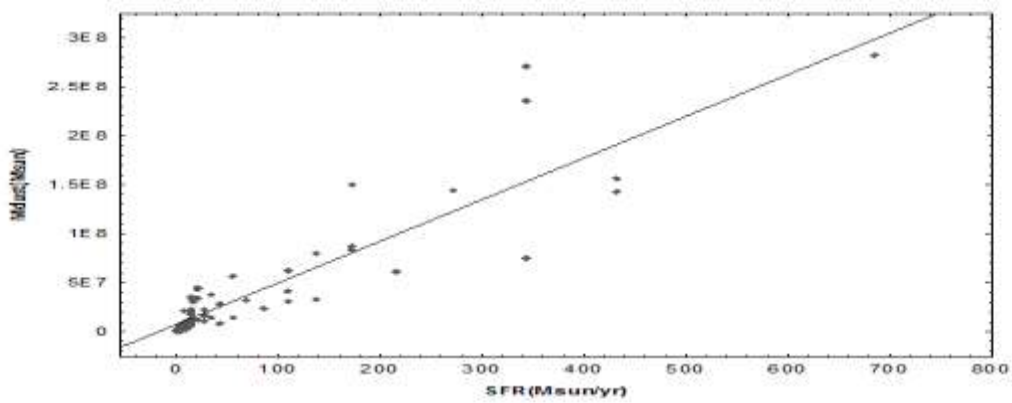

Figure 6- The mass dust M_{dust} versus star formation rate in ($M_\odot$ yr^{-1}).

The results of regression analysis show that the logarithmic ratio of L_{FIR}/MH_2 to $F1_{00}/F_{60}$ is apparently positive and well correlated (R~ 0.5) and that their relationship is not linear ($L_{FIR}/MH_2 \, \alpha \, F_{100}/F_{60}{}^{0.4\pm\ 0.09}$), as demonstrated in Figure-7a (left panel). This indicates that the Far- infrared luminosity for each unit of the molecular gas mass is an indicator of the star formation rate as it is directly related to infrared luminosity, where star formation activity occurs within the molecular clouds as an indication of the cold dust temperature component (which is mainly mixed with the HI gas).The parameter log (F_{100}/F_{60}) is introduced because the real situation is more complicated and because it provides a reliable indication of the dust temperature between 26.37 K^0 and 55.76 K^0 which is based on the power-law emission adopted (i.e. $B_\lambda \, \alpha \, \lambda^n$, with n=0).

Figure-7b (right panel) reveals the variation of the cold dust temperature with the parameter (F_{100}/F_{60}). These results are consistent with previously reported findings [1].

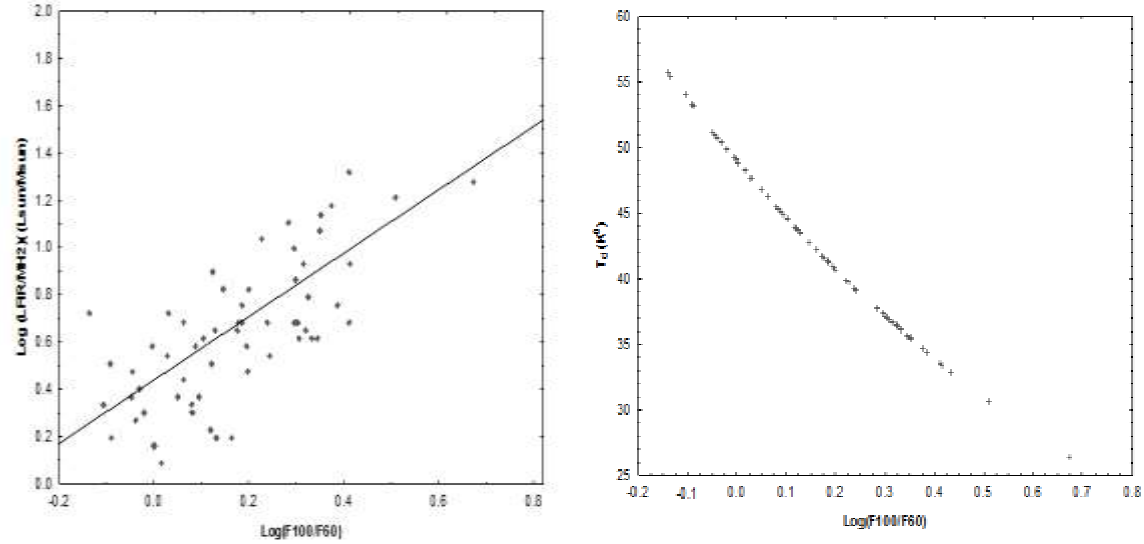

Figure 7- (a) The relationship between ratio L_{FIR}/MH_2 in ($L_\odot/M_\odot$) and the flux ratio F_{100}/F_{60}. ***(b)*** The cold dust temperature T_d (K^0) as a function of ratio $F1_{00}/F_{60}$ for n=0.

Conclusion

On the basis of our statistical analysis, we infer that the molecular and atomic hydrogen contents are related to a linear relationship (Slope ~ 1) with the hotter dust mass, but the correlation in the case of molecular gas is stronger. This refers to the abundance of dust in the case of atomic and molecular gas produced in the Far-infrared wavelengths band (60 -100) µm. We found, based on the statistical analysis, that the average value of the ratio MH_2/M_{dust} is $1.8x10^{10}$ $M_\odot$. The results also indicated that far-infrared emission has a tight relationship with all variables, which illustrates the presence of recent starburst which is in turn an indicative of the star formation activity, as Far-infrared luminosity (L_{FIR}) is related with the mass of molecular hydrogen and star formation rate (SFR_{FIR}) in this type of galaxies directly.

We observed the difference of the correlation in FIR- infrared luminosity and CO luminosity with other parameters in our sample, that is, the mean value of L_{FIR} (L_{FIR} ~10^{11} $L_\odot$) is larger than that in L_{CO} ($L_{co} \approx 10^9$ $L_\odot$). This work also revealed that the actual meaning of the gas is indicated by the total mass of cold gas and CO to FIR emission spectra that are related with the molecular hydrogen material MH_2, while increasing Far-infrared luminosity leads all these parameters to increase. The ratio F_{100}/F_{60} is an indicator of the cold dust temperature T_d. The value of dust temperature was in the range of 26.37-55.76 K^0. Depending on the power-law emission ($B_\lambda \, \alpha \, \lambda^n$), it was found that the increase in cold dust temperature is associated with increasing the star formation activity.

References

1. Oosterloo, T. **2010.** Early-type galaxies in different environments: an HI view, *Mon. Not. R. Astron. Soc.*, **409**: 500–514,

2. Kamenetzky, J., Rangwala, N., Glenn, J., Maloney, P. R. and Conley, A. **2016**. *L*CO /*L*FIR Relations with CO Rotational Ladders of Galaxies Across The HERSCHEL SPIRE Archive. *The Astrophysical Journal*, **829**: 93-109.
3. Buat, V., Boselli, A., Gavazzi, G., and Bonfanti, C. **2002**. Star formation and dust extinction in nearby star forming and starburst galaxies. *Astronomy & Astrophysics*, **383**: 801-812.
4. Boselli, A., Lequeux, J. and Gavazzi, G. **2002.** Molecular Gas in Normal Late-Type Galaxies. *Astronomy & Astrophysics*, **384**: 33–47.
5. Yali, Sh. **2019**. Star Formation and ISM Properties in Host Galaxies of Three Far-infrared Luminous Quasars at z ∼ 6. *The Astrophysical Journal*, **876**(2): 1-11.
6. Al Najm, M. N., Polikarpova, O. L., and Shchekinov, Yu. A. **2016.** Ionized Gas in the Circumgalactic Vicinity of the M81 Galaxy Group. *Astronomy Reports*, **60**(4): 389–396,
7. Andreani, P., Casoli, F. and Gerin, M. **1995**. CO, HI and cold dust in a sample of IRAS galaxies. *Astronomy & Astrophysics*, **300:** 43-57.
8. Vis, P. De. **2019.** A Systematic Metallicity Study of Dust Pedia Galaxies Reveals Evolution in the Dust-to-Metal Ratios. *Astronomy & Astrophysics*, **623**: A5-A30.
9. Kandalyan, R. A. **2003**. The Cold Gas Properties of Markarian Galaxies. *Astronomy & Astrophysics*, **398**: 493–499.
10. https://ned.ipac.caltech.edu
11. Al Najm, M. N., Rashed, Y.E. and AL-Dahlaky, H. H. **2018.** Spectral Multi-Wavelength Properties of a RBSC-NVSS Observation for a Sample of Active Galaxies. *Indian Journal of Natural Sciences*, **9**(51): 15729-15740.
12. Rashed, Y. E., Al Najm, M. N. and Al Dahlaki, H. H. **2019.** Studying the Flux Density of Bright Active Galaxies at Different Spectral Bands. *Baghdad Science Journal*, **16**(1): 230-236.
13. Kana, M., Kazuo, S.,Yoshimasa, W. and Nario, K. **2012.** Detection of CO (J = 1−0) Emission from Barred Spiral Galaxies at z ~ 0.1. *Astronomical Society of Japan (PASJ)*, **64:** 55-64.
14. Tutui, Y., Sofue, Y., Honma, M., Ichikawa, T. and Wakamatsu, K-I. **2000.** CO Observations of Luminous IR Galaxies at Intermediate Redshift. *Astronomical Society of Japan (PASJ)*, **52**: 803-820.
15. Martin, J. M., Bottinelli, L., Dennefeld, M. and Gouguenheim, L. **1991**. An 18-cm OH and 21-cm H I survey of luminous far-infrared galaxies. II - H I properties. *Astronomy and Astrophysics*, **245**(2): 393-417.
16. Solomon, P. M. and Sage, L. J. **1988.** Star-formation rates, molecular clouds, and the origin of the far-infrared luminosity of isolated and interacting galaxies. *The Astrophysical Journal*, Part 1, **334**: 613-625.
17. Junko U. **2014**. Cold Molecular Gas in Merger Remnants. I. Formation of Molecular Gas Disks. *The Astrophysical Journal Supplement Series*, **214:** 1-29.
18. Solomon, P. M. and Vanden Bout, P. A. **2005**. Molecular Gas at High Redshift. *Annual Review of Astronomy and Astrophysics,* **43**: 677-725.
19. Chen, Ch.-Ch. et al. **2017.** A Spatially Resolved Study of Cold Dust, Molecular Gas, HII Regions, and Stars in the z = 2.12 Submillimeter Galaxy ALESS67.1. *The Astrophysical Journal*, **846**: 108-133.
20. Bregman, J. N., Snider, B. A., Grego L. and Cox, C. V. **1998.** FAR-Infrared Emission from E And E/S0 Galaxies. *The Astrophysical Journal*, **499:** 670-676.
21. Vis De, P. et al. **2019.** A Systematic Metallicity Study of Dust Pedia Galaxies Reveals Evolution in the Dust-to-Metal Ratios. *Astronomy & Astrophysics*, **623**: A5-A30,
22. Judith, S. Y., Shuding, X., Jeffrey D. P. K. and Walter L. R. **1989.** Global Properties of Infrared Bright Galaxies. *The Astrophysical Journal Supplement Series*, **70**: 699-722.
23. Yu-Qing L. and Fu-Yan B. **2005.** Correlations among Multiwavelength Luminosities of Star-Forming Galaxies. *Mon. Not. R. Astron. Soc*. **358**: 1231–1239.